

New features in the radio-emission of very inclined air-showers

Simon Chiche,^{a,*} Chao Zhang,^{c,b,i} Kumiko Kotera,^{a,j} Tim Huege,^{c,j} Krijn D. de Vries,^f Felix Schlüter^{c,h} and Matias Tueros^{d,e,a}

^a*Sorbonne Université, CNRS, UMR 7095, Institut d'Astrophysique de Paris, 98 bis bd Arago, 75014 Paris, France*

^b*Kavli institute for astronomy and astrophysics, Peking University, Beijing, China*

^c*Institute for Astroparticle Physics (IAP), Karlsruhe Institute of Technology, Karlsruhe, Germany*

^d*IFLP - CCT La Plata - CONICET, Casilla de Correo 727 (1900) La Plata, Argentina*

^e*Depto. de Física, Fac. de Cs. Ex., Universidad Nacional de La Plata, Casilla de Correo 67 (1900) La Plata, Argentina*

^f*Vrije Universiteit Brussel (VUB), Dienst ELEM, Pleinlaan 2, B-1050, Brussels, Belgium*

^j*Astrophysical Institute, Vrije Universiteit Brussels, Pleinlaan 2, 1050 Brussels, Belgium*

^g*Sorbonne Université, Université Paris Diderot, Sorbonne Paris Cité, CNRS, Laboratoire de Physique Nucléaire et de Hautes Energies (LPNHE), Paris, France*

^h*Universidad Nacional de San Martín, Instituto de Tecnologías en Detección y Astropartículas, Buenos Aires, Argentina*

ⁱ*Department of Astronomy, School of Physics, Peking University, Beijing, China*

E-mail: simon.chiche@iap.fr

To probe the sources of ultra-high energy cosmic-rays, the next generation of radio experiments such as GRAND, BEACON and AugerPrime Radio are now focusing on the detection of air-showers arriving with very inclined trajectories. These inclined showers have a large footprint that allows us to instrument large surfaces at low costs, but their radio emission exhibits numerous features that differentiate them from vertical ones. Using Monte-Carlo simulations, we evidence here two major novel features of cosmic-ray inclined showers: a significant drop of more than one order of magnitude in the geomagnetic emission amplitude and a new polarization pattern. We explain the former by a coherence loss in the radio emission of inclined air-showers, while the latter possibly indicates a synchrotron emission becoming relevant at large zenith angles. These two effects depend both on the magnetic field amplitude and are challenging to describe with the existing interpretations of the radio emission but could affect the detection and reconstruction strategies of next generation experiments.

*9th International Workshop on Acoustic and Radio EeV Neutrino Detection Activities - ARENA2022
7-10 June 2022
Santiago de Compostela, Spain*

*Speaker

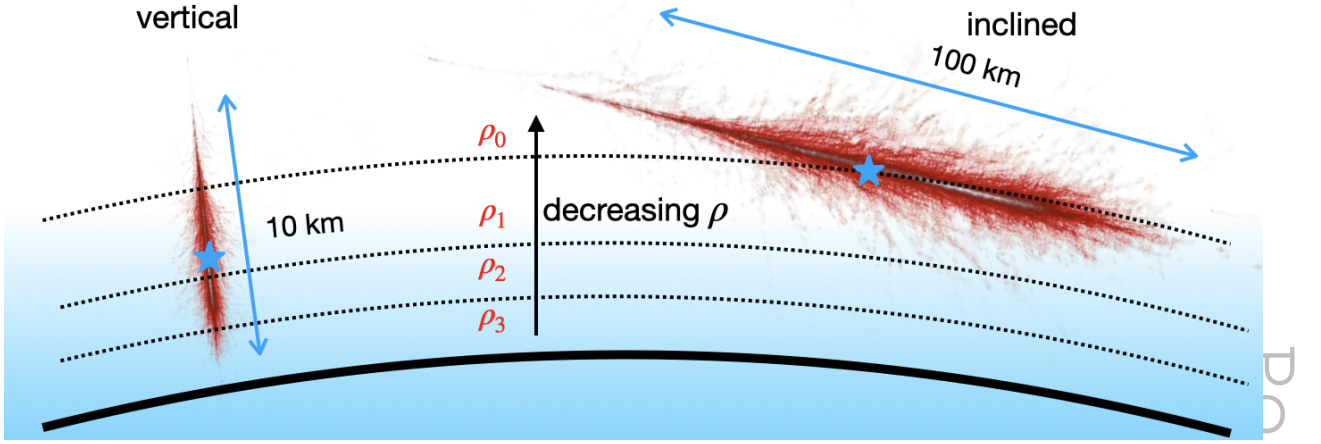


Figure 1: (Not to scale) Sketch of a vertical and an inclined air-shower. The blue star indicates the X_{\max} position of each shower. Inclined air-showers develop at higher altitude, hence lower density in the atmosphere and over longer distances than vertical ones. The sketch also shows that Earth curvature and the asymmetry of the atmospheric density around the shower axis should be considered for inclined air-showers.

1. Introduction

Radio detection of high-energy astroparticles has been extensively studied over the past decade. Experimental progresses in cosmic-ray detection from CODALEMA [1], LOPES [2], AERA [3] and LOFAR [4] fed the development of accurate Monte-Carlo simulations and of theoretical models, providing a deep understanding of the radio emission processes [5, 6]. The radio emission from vertical showers is now well understood and can be interpreted as the coherent sum of two main mechanisms: the geomagnetic emission, coming from the deflection of charged particles in the shower by the Earth’s magnetic field and the time variation of the resulting transverse current; and the charge-excess emission coming from the accumulation of negative charges in the shower front due to the ionization of air-atoms. The objective of the community is now to increase the sensitivity and to target other messengers, gamma-rays and neutrinos, at ultra-high-energy (UHE). This motivates the development of next generation experiments with gigantic detection surfaces and more efficient detection methods with a focus on radio techniques to address the low fluxes at UHE [7, 8]. Inclined air-showers are particularly well-suited for this purpose as their large radio footprints allow us to sample the signal with sparse arrays and cover large surfaces at low costs. Yet, their radio emission exhibits numerous features that differentiate them from vertical showers making their understanding challenging with the existing theoretical models [9, 10]. In Section 2 we present the main characteristics of inclined showers. We then evidence in Section 3 two new features of inclined air-shower radio emission: a suppression of the radiated energy and a new polarization signature at low densities and high magnetic field amplitude. Eventually in Section 4, we discuss how the current theoretical models should be refined to account for these two effects that we link respectively to a loss of coherence and a synchrotron component.

2. The challenge of inclined air-showers

When a particle cascade develops in the atmosphere, the total number of particles increases until it reaches a maximum, and then decreases. The atmospheric grammage X_{\max} at which the

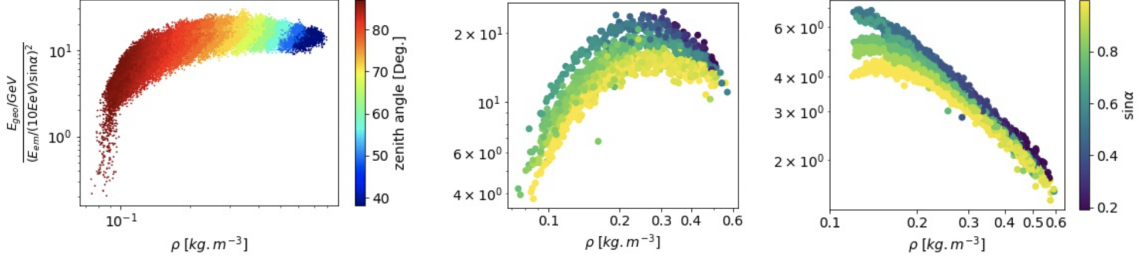


Figure 2: (Left) Full band radiated geomagnetic energy as a function of air-density from ZHAireS simulations with GRAND magnetic field configuration ($B = 55 \mu\text{T}$, $i = 60.79^\circ$). The colors code for the zenith angle. When going from high to low air-density, the radiated energy first increases up to $\rho_{\text{air}} = 0.3 \text{ kg m}^{-3}$ ($\theta \sim 70^\circ$) and then drops by almost 1.5 order of magnitude for the lowest densities (the most inclined showers). (Middle) Radiated energy, filtered in the 50 – 200 MHz band, as a function of air-density from CoREAS simulations with GRAND magnetic field. The colors code for $\sin \alpha$, with α the geomagnetic angle. The plot shows a similar trend to the results with ZHAireS simulations, i.e., an increase of the radiated energy followed by a drop at the lowest densities. The colors attest of a deviation from a scaling of the radiated energy as $\sin^2 \alpha$. (Right) Radiated energy as a function of air-density from CoREAS simulations with AERA magnetic field configuration ($B = 24.6 \mu\text{T}$, $i = -35.2^\circ$) and frequency band (30 – 80 MHz). The plot shows almost no cut-off at low densities and the radiated energy roughly scales in $\sin^2 \alpha$.

maximal number of particles is reached depends mainly on the particle nature and not on its arrival direction. As a consequence, inclined cosmic-ray air-showers will develop in higher, hence lower density atmosphere than vertical ones. This is illustrated in Fig. 1, where we highlight some differences between vertical and inclined showers that are relevant in our framework. It can be seen that inclined showers develops over much longer distances than vertical ones, resulting in a more diluted signal. This long development also implies that Earth curvature has to be taken into account when modeling the atmosphere and setting the antennas positions on ground. The inclined shower trajectory will also create an asymmetry of the radio footprint related to a different integrated refractive index and time arrivals of the signal between "early" antennas (located below the shower axis) and "late" antennas (above the shower axis) [11, 12]. Eventually, the lower density for inclined showers should impact the radio emission processes as discussed in [9, 10, 15]. In the next Section we aim at characterizing quantitatively the impact of air-density on the radio emission with Monte-Carlo simulations.

3. Radio signal dependency with air-density

3.1 Evidence for a suppression of the radiated energy of inclined air-showers

To compute the radio-signal dependency with air-density, we calculated with ZHAireS Monte-Carlo simulations [13] the radiated energy for showers with various inclination. We used a set of $\sim 10\,000$ showers with antennas on a star-shape layout, with zenith angle θ between $[40^\circ - 80^\circ]$, various azimuth angles ϕ and primary particle energy \mathcal{E} between $[0.1 - 4]$ EeV. The magnetic field amplitude is set to $B_{\text{geo}} = 55 \mu\text{T}$ and its inclination to $i = 60.79^\circ$ following the values at the GRAND experiment candidate site, in Dunhuang, China.

As discussed in [9], for inclined showers, the charge-excess contribution to the radio signal becomes negligible relatively to the geomagnetic one. We can therefore assume that the radiated

geomagnetic energy, $E_{\text{rad geo}}$ is an accurate proxy for the total radiated energy by the air-shower. $E_{\text{rad geo}}$ is calculated following the method proposed in [14], i.e., by integrating the $\mathbf{v} \times \mathbf{B}$ component of the radio energy fluence $f_{\mathbf{v} \times \mathbf{B}} = \epsilon_0 c \Delta t |E_{\mathbf{v} \times \mathbf{B}}|^2$ (with E , the electric field integrated over the time window of length Δt , ϵ_0 , the vacuum permittivity and c the speed of light in vacuum) using antennas located on the $\mathbf{v} \times (\mathbf{v} \times \mathbf{B})$ axis and assuming a radial symmetry of the radio signal. Finally, we divide the result by $\mathcal{E}^2 \sin^2 \alpha$, (with α , the geomagnetic angle and \mathcal{E} the shower electromagnetic energy) to correct the result from any dependency with the primary energy and azimuth angle. We get:

$$E_{\text{geo}}^{\text{rad}}(\epsilon, \Phi, \theta) = \frac{2\pi\epsilon_0 c \Delta t}{\mathcal{E}^2 \sin^2 \alpha} \int_0^{+\infty} |E_{\text{geo}}(r)|^2 r dr \quad (1)$$

Here, $r dr$ (with r , the distance of a given antenna from the shower core) can be re-expressed as $D_{X_{\text{max}}}^2 \omega d\omega$ with $D_{X_{\text{max}}}$, the distance between X_{max} and the shower core, and ω , the angular deviation to the shower axis from X_{max} , such as $\tan(\omega) \sim \omega = r/D_{X_{\text{max}}}$. It should be noted that rigorously, the X_{max} -observer distance should be used instead of the X_{max} -shower core distance. However, in practice the radio footprint extends only to small viewing angles (\sim up to 3°) and we can thus assume that both quantities are roughly equal.

The result is displayed as a function of air-density or zenith angle, on the left-hand of Fig. 2, for the full band electric field. It can be seen that when going from high to low densities, the radiated energy first slightly increases (for θ between 40° to 70°) and then decreases (for θ above 70°), with a cut-off of more than 1.5 orders of magnitude for the most inclined showers. This result is confirmed with CoREAS simulations [16] on the middle panel of Fig. 2, where a similar behavior is observed in the GRAND frequency band (50 – 200 MHz). On the other hand, in the right-hand of Fig. 2, we present the radiated energy as a function of air-density using this time the magnetic field configuration and frequency band of the Auger site AERA in Malargüe ($B = 24.6 \mu\text{T}$, $i = -35.2^\circ$). It should be noted that although different frequency band are depicted on the 3 plots, no significant deviation from the filtering is expected between the full band, GRAND and Auger case, as the peak of the radio signal spectrum (around tens of MHz) is included in each of the considered band. In the right-hand of Fig. 2, it can be seen that when lowering the density, the radiated energy almost always increases and only a mild cut-off is observed for $\rho < 0.1 \text{ kg m}^{-3}$. This decrease and the associated cut-off of the radiated energy for GRAND magnetic field values are unexpected features that are not predicted by any existing theoretical description of the radio emission. Indeed, in the classical picture, one would expect that when lowering the density it would increase the mean free path of collision of positrons and electrons in the shower, resulting in a stronger current and a stronger geomagnetic emission. However, our results suggest that for low air-densities coupled with high magnetic field values, the current theoretical descriptions of the radio emission are no longer valid and should be refined to account for these new effects.

3.2 Evidence for a new polarization signature

We also studied, with Monte-Carlo simulations, how the polarization should be modified for inclined air-showers. On the left panel of Fig. 3 we represented, from ZHAireS simulations, the $\mathbf{v} \times (\mathbf{v} \times \mathbf{B})$ component of the full band electric field ($E_{\mathbf{v} \times \mathbf{v} \times \mathbf{B}}$), for a shower with zenith angle $\theta = 38^\circ$. As the transverse current from the geomagnetic emission is polarized along the $-\mathbf{v} \times \mathbf{B}$ direction, the only contribution to $E_{\mathbf{v} \times \mathbf{v} \times \mathbf{B}}$ should come from the charge-excess emission. This

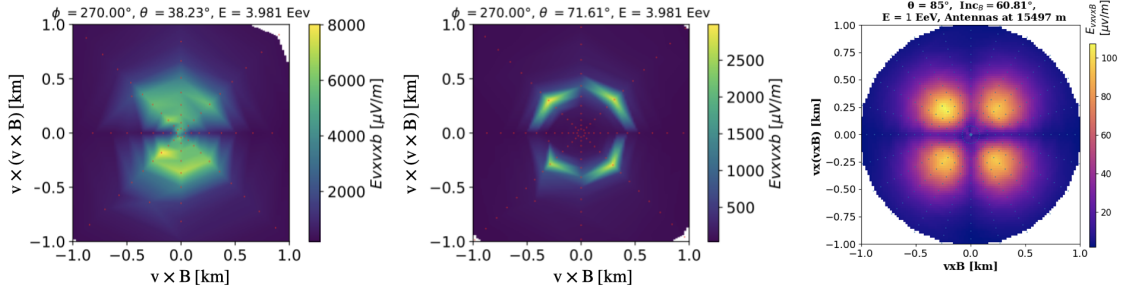


Figure 3: Projected component of the full band peak electric field along $\mathbf{v} \times (\mathbf{v} \times \mathbf{B})$ from Monte-Carlo simulations for (*left*), a ZHAireS simulation with zenith angle $\theta = 38^\circ$, (*middle*), a ZHAireS simulation with zenith angle $\theta = 72^\circ$ and (*right*), a CoREAS simulation with zenith angle $\theta = 85^\circ$. The results are shown in the $[\mathbf{v} \times \mathbf{B}; \mathbf{v} \times (\mathbf{v} \times \mathbf{B})]$ plane, perpendicular to the shower axis, where \mathbf{v} and \mathbf{B} are unitary vectors. The left-hand plot shows a pattern that follows the usual projection of the charge excess emission along the $\mathbf{v} \times (\mathbf{v} \times \mathbf{B})$ axis. The middle and the right-hand plot however, show a polarization pattern that cannot be described by the existing theoretical models of the radio emission and hints toward a new emission taking over the charge excess for inclined air-showers.

is confirmed by the footprint that follows the expected pattern for the $\mathbf{v} \times (\mathbf{v} \times \mathbf{B})$ projection of the charge excess, i.e., an emission that is peaked along the $\mathbf{v} \times (\mathbf{v} \times \mathbf{B})$ axis and reaches 0 along the $\mathbf{v} \times \mathbf{B}$ axis. On the middle and right panel of Fig. 3, we also represent the full band $E_{\mathbf{v} \times \mathbf{v} \times \mathbf{B}}$, but respectively for ZHAireS and CoREAS simulations of a shower with zenith angle $\theta = 72^\circ$ (respectively $\theta = 85^\circ$). Here we can see, with both simulations, that the emission follows a "clover-leaf pattern", i.e., is peaked on the diagonal axes and vanishes along the $\mathbf{v} \times \mathbf{B}$ and $\mathbf{v} \times (\mathbf{v} \times \mathbf{B})$ directions. This pattern, that is observed for inclined air-shower simulations, can not be described by the current theoretical descriptions of the radio emission assuming only a transverse current and charge excess contribution. It can only be explained by a weaker charge excess emission (as discussed in [9]) and the emergence of new type of emission dominant over the charge excess for low air-densities. This new polarization pattern could potentially come from synchrotron emissions as suggested by geo-synchrotron models which predicted a clover-leaf like pattern, similar to the one observed in Fig. 3, in the GHz band for vertical showers [19]. In the next Section, we propose a model to characterize this new emission.

4. Refined modeling of the radio emission

In the previous section, we evidenced, with Monte-Carlo simulations, two new effects in the radio emission of air-showers for low air-density, ρ_{air} , and high Earth magnetic field amplitude, B_{geo} : a suppression of the radiated energy and a new polarization pattern. These effects become significant for inclined ($\theta \gtrsim 70^\circ$) air-showers, but are not predicted by any existing theoretical description of the radio emission. In this section, we propose how the current models of the radio emission should be refined to account for these new effects.

4.1 Conditions for a coherent signal in the radio emission of air-showers

As discussed in Section 3.1, the suppression of the radiated energy of inclined air-showers appears to be linked to a low air-density, combined with a high magnetic field amplitude. This suggests that it could be related to the shower lateral extent, L_{lat} , which itself depends on both of

these parameters. Indeed, lowering the air-density should increase the mean free path of collision of electrons and positrons, while increasing the magnetic field should enhance the deflection, both resulting in a larger shower lateral extent. If we assume that the radio emission is emitted around X_{\max} , then we can construct with L_{lat} the spatial coherence length given by:

$$L_c = \frac{\lambda D_{X_{\max}}}{L_{\text{lat}}}, \quad (2)$$

where λ is the wavelength of the emission and $D_{X_{\max}}$, the distance between X_{\max} and the shower core. This condition arises from the fact that if particles in a plane perpendicular to the shower axis at X_{\max} radiate in phase, then the only phase difference at the observer position will come from the different particle locations, i.e., from the plane lateral extension. The spatial coherence length hence allows us to quantify if an observer located at $D_{X_{\max}}$ from the plane, will receive radiations in phase or not, depending on whether we have $L_{\text{lat}} < L_c$ (for a coherent emission, constructive interferences) or $L_{\text{lat}} > L_c$ (for an incoherent emission).

In Eq. 2, $D_{X_{\max}}$ can be computed from Monte-Carlo simulations, while L_{lat} needs to be determined. Using the formalism of [17], we can express the transverse acceleration of particles in the shower as $d^2x_t/dt^2 = c^3 e B / [\epsilon_e \exp(-t/\tau)]$, with x_t , the particle transverse position (orthogonal to the shower axis), $\tau = l_{\text{rad}}/c$ the Bremsstrahlung energy loss timescale and $l_{\text{rad}} = X_0/\rho_{\text{air}} \sim 3.67 \times 10^3 \text{ m } (\rho_{\text{air}}/1 \text{ g cm}^{-3})^{-1}$, where $X_0 = 36.7 \text{ g cm}^{-2}$ is the electronic radiation length. Integrating the transverse acceleration as a function of time we get $x_t(t) = \tau^2 c^3 e B (e^{t/\tau} - 1 - t/\tau) / \epsilon_e$. The shower lateral extent L_{lat} is then derived as $L_{\text{lat}} = 2x_t(t = \tau)$, where the factor 2 account for the deflection of both positrons and electrons. We represent L_{lat} and the coherence length L_c on the left panel of Fig. 4. We can see that for $\rho_{\text{air}} \gtrsim 0.3 \text{ kg m}^{-3}$, i.e. for $\theta < 75^\circ$, we have $L_{\text{lat}} < L_c$ and therefore expect coherent emission. However, for more inclined air-showers, i.e., for $\rho_{\text{air}} \lesssim 0.3 \text{ kg m}^{-3}$ ($\theta > 75^\circ$) we have a transition to a regime where $L_{\text{lat}} > L_c$ and incoherent emission is expected. The transition from coherent to incoherent emission matches well with the suppression of the radio energy and suggest that for inclined showers an attenuation in e^{-L_{lat}/L_c} is expected.

4.2 Conditions for synchrotron emission in the radio emission of air-showers

For low air-densities and high magnetic field values we also expect charged particles in the shower to undergo an enhanced magnetic deflection with associated synchrotron emission. We use the theoretical framework developed by C. James in [18] and assume that a non negligible synchrotron emission is expected if particles can radiate before losing their energy, i.e., for $l_{\text{synch}} < l_{\text{rad}}$, with l_{rad} , the Bremsstrahlung energy loss length which is given by $l_{\text{syn}} \sim 1157 \text{ m } (\epsilon_e/88 \text{ MeV})^{2/3} (B/50 \mu\text{T})^{-2/3} (\nu/80 \text{ MHz})^{-1/3}$, the synchrotron cooling length derived in [18]. Both lengths are represented in the right panel of Fig. 4 as a function of frequency for GRAND and Auger magnetic field values (respectively $55 \mu\text{T}$ and $24.6 \mu\text{T}$). The $\sin \alpha$ value (with α the geomagnetic angle) is set to 1 for GRAND site and to 0.5 for Auger site, according to the values favored by the magnetic field inclination at each location. Also, as we are looking to the dynamics of particles around X_{\max} , the particle energy \mathcal{E}_e , is set to the critical energy $E_c \sim 80 \text{ MeV}$. We can see on Fig. 4 that for frequencies around 50 – 200 MHz, the model from [18] predicts, with GRAND magnetic field value, a transition to a regime where a non negligible synchrotron emission is expected for inclined air-showers (for $\theta \gtrsim 75^\circ$). However, for the same zenith angle,

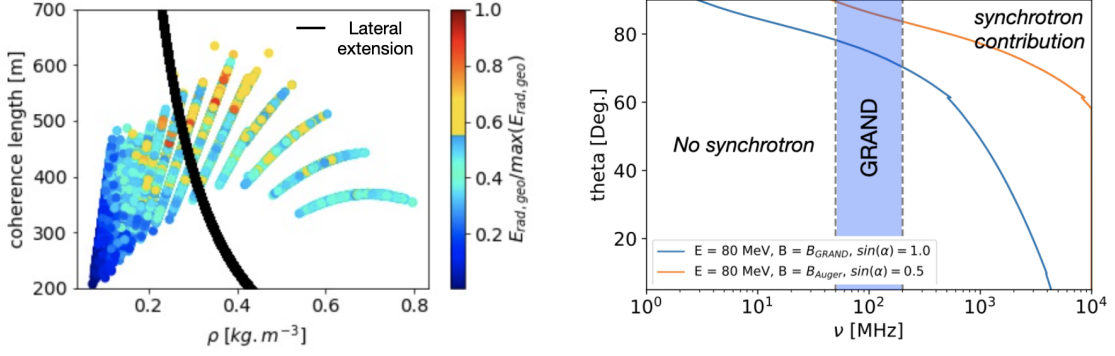


Figure 4: (Left) Shower lateral extent (L_{lat}) and spatial coherence length (L_c), as a function of air-density. The color code shows the normalized radiated energy. The plot shows that we have $L_{\text{lat}} < L_c$ and expect a coherent emission for $\rho_{\text{air}} \gtrsim 0.3 \text{ kg m}^{-3}$ and $L_{\text{lat}} > L_c$, i.e., expect an incoherent emission for $\rho_{\text{air}} \lesssim 0.3 \text{ kg m}^{-3}$. This result is consistent with the radiated energy which drops significantly once the coherence is lost. (Right) Transition lines from a regime with no expected synchrotron component to a regime with non negligible synchrotron contribution for GRAND (blue line) and Auger (orange line) magnetic field configurations. The plot shows that for GRAND magnetic field configuration, the transition to a regime with non negligible synchrotron contribution is expected for $\theta \gtrsim 75^\circ$ at frequencies between 50 – 200 MHz. On the other hand, for Auger, frequencies of $\sim 1 \text{ GHz}$ are required to see this transition with the same zenith angle.

frequencies of $\sim 1 \text{ GHz}$ are needed to observe the same transition with Auger magnetic field strength and inclination. This suggests that the new polarization pattern observed for inclined showers in Section 3.2, with Monte-Carlo simulations using GRAND magnetic field configuration, could be well explained by our synchrotron model but should be hardly visible with Auger magnetic field.

5. Conclusion

Inclined cosmic-ray air-showers develop higher in the atmosphere than vertical ones and show numerous features that make their understanding more challenging. In this study, we explored, with ZHAireS and CoREAS Monte-Carlo simulations, the radio emission of these inclined showers. This allowed us to evidence two major novel features: a suppression of the radiated energy and the emergence of a new polarization pattern for low air-densities and high magnetic field values. We then developed a refined modeling of the air-shower radio emission to account for these new effects that we linked respectively to: a loss of coherence in the radio signal and an additional synchrotron contribution for inclined air-showers. Our results are summarized in Fig. 5, where the characteristic

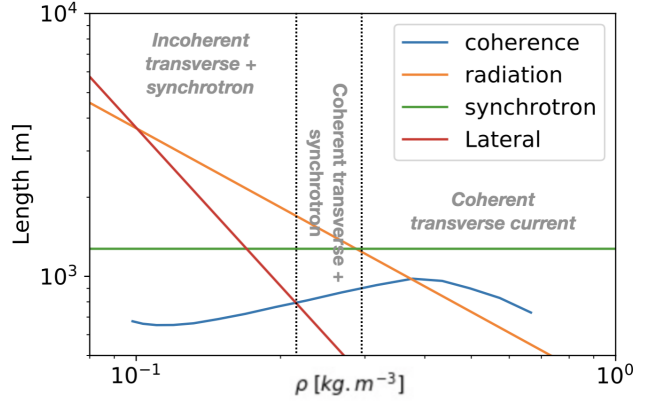


Figure 5: Characteristic lengths of relevant physical observables in air-showers. Three distinct regimes can be identified: (1) at high densities we expect a coherent transverse current emission, (2) at intermediate densities, the radio emission combines a coherent transverse current emission with a synchrotron-like pattern, (3) at the lowest densities, an incoherent emission is expected.

lengths of the various processes at play are displayed. This allowed us to evidence 3 distinct regimes as a function of air-density: (1) at high densities we retrieve a coherent transverse current emission as predicted by the former models, (2) at intermediate densities we find an additional coherent synchrotron contribution to the transverse current emission, (3) at the lowest densities we find that an incoherent radio emission is expected. These regimes are highly dependent on the magnetic field amplitude and have strong implications: (1) they show that the current description of radio signals made of a transverse current and a charge excess contribution only is no longer valid for inclined air-showers; (2) they show that the radio emission cut-off is site dependent and could be used to either enhance the cosmic-ray detection or attenuate it, depending on the B_{geo} value. Particularly, as neutrino showers develop deeper in the atmosphere than cosmic-rays, their radio emission should not be subject to any cut-off. As a consequence, choosing a site with high magnetic field value could be interesting to perform cosmic-ray/neutrino discrimination.

6. Acknowledgements

The authors would like to thank Marion Guelfand, Olivier Martineau-Huynh, Pragati Mitra, Simon Prunet, Olaf Scholten and Washington R. Carvalho Jr for the fruitful discussions on the radio cut-off, Nikolaos Karastathis for his valuable input on the synchrotron emission with CORSIKA and the organizers of the ARENA conference for setting the event.

References

- [1] D. Charrier *et al*, *Astroparticle Physics* **113**, 6–21 (2019).
- [2] W.D. Apel *et al*, *The European Physical Journal C* **81**, (2021).
- [3] A. Aab, *et al*, *Physical Review D*, **89**, pp.052002. (2014).
- [4] A. Corstanje *et al*, *Astroparticle Physics* **61**, 22–31 (2015).
- [5] T. Huege, *Physics Reports* **620**, 1–52 (2016).
- [6] F. Schroeder, *Progress in Particle and Nuclear Physics* **93**, 1–68 (2017).
- [7] J. Álvarez-Muñiz *et al*, *Science China Physics, Mechanics & Astronomy* **63**, (2019).
- [8] B. Pont *et al*, *PoS ICRC2019*, 395 (2019).
- [9] S. Chiche *et al*, *Astroparticle Physics* **139**, 102696 (2022)
- [10] F. Schlüter and T. Huege, arXiv <https://arxiv.org/abs/2203.04364>, (2022).
- [11] F. Schlüter *et al*, *The European Physical Journal C* **80**, 643 (2022).
- [12] T. Huege *et al*, arXiv <https://arxiv.org/abs/1908.07840>, (2019).
- [13] Jaime Alvarez-Muñiz *et al*, *Astroparticle Physics* **35**, 6, 325–341, (2012)
- [14] C. Glaser *et al*, *Journal of Cosmology and Astroparticle Physics* **2016**, 09, 024–024, (2016)
- [15] S. Chiche *et al*, arXiv <https://arxiv.org/abs/2202.05886>, (2022).
- [16] T. Huege *et al*, arXiv <https://arxiv.org/abs/1301.2132>, (2013).
- [17] O. Scholten *et al*, *Astroparticle Physics* **29**, 2, 94–103, (2008)
- [18] C. James, *Physical Review D* **105**, 2 (2022)
- [19] T. Huege and H. Falcke, *Astronomy & Astrophysics* **430**, 3, 779–798, (2004)
- [20] J. Hörandel, *Proceedings of 37th International Cosmic Ray Conference — PoS(ICRC2021)*, (2021).